Chapter-IV

4.1 Introduction

As discussed in Chapter III (Sections 3.5.2.2 and 3.5.2.3), the MPB region of $Bi(Ni_{1/2}Ti_{1/2})O_3$-$PbTiO_3$ exhibit a monoclinic (Pm) phase similar to well-known MPB ceramics like PZT [Singh et al. (2007)] and PMN-PT [Singh and Pandey (2003)]. However, the characteristic splitting in the diffraction profile corresponding to monoclinic phase are not resolved well in the laboratory XRD data. In the present work, we have discovered an electric field induced crystallographic phase transition in the pseudocubic composition of multiferroic (1-x)BNT-xPT solid solution. The x-ray diffraction profiles are seen to be clearly splitted after electric field poling and confirm the monoclinic structure [Pandey and Singh (2014)]. Electric field induced phase transition has been investigated earlier in important MPB ceramics such as $PbZr_{1-x}Ti_xO_3$ (PZT) [Guo et al. (2000); Schonau et al. (2007)], (1-x)$Pb(Mg_{1/3}Nb_{2/3})O_3$-x$PbTiO_3$ [Guo et al. (2003); Li et al. (2008)] in the compositions close to MPB. Around MPB, the crystal structure is very sensitive and may get modified by small stimuli like electric field, pressure or compositional variations. We find that the electric field induced phase transition in 0.65BNT-0.35PT (pseudocubic phase) is also accompanied by significant change in the unit cell volume and results in large microscopic lattice strain (1.6%) in c-direction. This suggests that apart from the MPB compositions, the pseudocubic compositions close to MPB can also be used for getting strain for micropositioner and actuator applications. The giant electromechanical response in pseudocubic compositions close to MPB are

resulting from electric field induced structural transition. The present discovery is expected to stimulate a systematic study of the electric field induced phase transitions and its correlation to the electromechanical responses in the various MPB solid solutions. We have also investigated the electric filed induced structural changes in the MPB and tetragonal compositions. We find significant domain extension and domain reorientation after electric field poling in these compositions. We believe that this work will provide better understanding of the electric field induced phase transitions in multiferroic systems and will help in designing the novel devices.

This Chapter presents the results of electric field induced structural changes in cubic, MPB and tetragonal compositions of BNT-PT.

4.2. Experimental Details

The samples were synthesized by traditional solid state ceramic method. The details of sample preparation are discussed in Chapter II. For the investigation of electric field induced phase transition, pellets of (1-x)BNT-xPT were electroded by coating silver paste on flat surfaces and fired at 500^0C for 5 minutes. The electroded pellets were poled in silicon oil bath cooling from 100^0C to room temperature under the applied DC electric fields of various strengths (5kV/cm, 10kV/cm, 15kV/cm, 20kV/cm and 30kV/cm). Electromechanical coupling coefficients were calculated by resonance-anti-resonance method [Jaffe et al. (1971)]. To record the XRD data from poled samples, silver electrode was gently removed from one surface of the pellet. Rietveld analysis and full profile fitting of XRD data was carried out using Fullprof-Suite.

4.3. Results and Discussion

We have selected three representative compositions; Pseudocubic (x=0.35), monoclinic (x=0.43) and tetragonal (x=0.50) to investigate the electric field induced phase transformations. As discussed in Chapter III (Section 3.5.2), for the compositions with x=0.35, all the profiles are singlet and reveal the cubic structure with space group $Pm\bar{3}m$. The structure of the compositions with x=0.50 is tetragonal with space group P4mm. The structure of the compositions with x=0.43 is monoclinic with space group Pm.

4.3.1. Composition Dependence of Planer Electromechanical Coupling Coefficient (K_p)

Planer electromechanical coupling coefficient (k_P) was calculated by resonance-antiresonance method using frequency vs impedance measurement on the poled pellets of BNT-xPT ceramics. Fig.4.1 shows the variation of electromechanical coupling coefficient (k_P) with compositions. As can be seen from this figure, a peak is observed around the composition with x=0.45 corresponding to MPB. Most surprisingly, significant value of k_p is obtained for the pseudocubic composition with x=0.35 also, which should not be observed for centrosymmetric cubic structure. This indicates that a phase transformation from centrosymmetric cubic to non-centrosymmetric ferroelectric phase takes place after poling. To confirm the electric field induced phase transition during poling, we carried out a detailed structural analysis of BNT-PT samples with x=0.35 poled at various electric field (E).

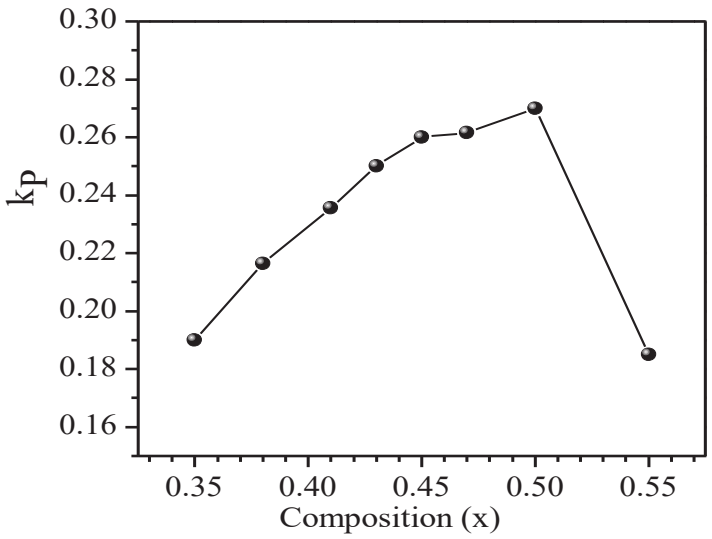

Fig.4.1 Variation of planer electromechanical coupling coefficient (k_P) with composition for (1-x)BNT-xPT solid solution.

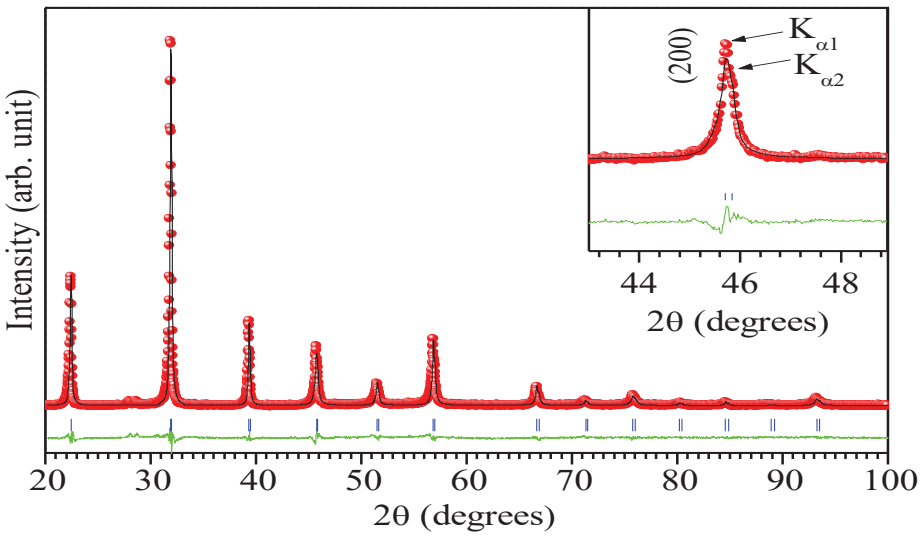

Fig.4.2 Experimentally observed (dots), theoretically calculated (continuous line) and their difference XRD profiles (continuous bottom line) obtained by Rietveld fit for unpoled 0.65BNT-0.35PT ceramics using cubic space group $Pm\bar{3}m$. The vertical tick-marks above the difference plot show the peak positions. Inset illustrates the quality of fit for the (200) profile.

4.3.2. Structure of 0.65BNT-0.35PT Poled at Various Electric Fields

Fig.4.2 depicts the observed, calculated and difference profiles for the composition with x=0.35 using space group $Pm\bar{3}m$ obtained by the Rietveld analysis. The fit between the observed and calculated profiles is quite good confirming the cubic structure. Inset to Fig.4.2 illustrates the goodness of fit for the (200) profile. After electric field poling all the XRD profiles split suggesting electric filed induced phase transformation to non cubic ferroelectric phase. The XRD profile of pellets poled at different poling field strength of 5kV/cm, 10kV/cm, 15kV/cm, 20kV/cm and 30kV/cm, are shown in Fig.4.3. The XRD profiles of the poled samples show clear splitting in contrast to the singlet character for the unpoled sample as shown in Fig.4.2. To illustrate it further, a comparison of the pseudocubic (110), (111) and (200) XRD profiles of the unpoled (continuous line) and poled ceramics (scattered dots) at the poling field of strength 20kV/cm is presented in Fig.4.4. As can be seen from this figure, there is drastic modification in the XRD profiles after poling. This clearly confirms the electric field induced phase transition in pseudocubic BNT-PT composition with x=0.35 as indicated by the appearance of electromechanical response also (see Fig.4.1). To determine the true symmetry of the new phase in poled sample, we carried out Rietveld profile matching analysis using different plausible space groups, i.e. rhombohedral $R\bar{3}m$, monoclinic Pm and monoclinic Cm.

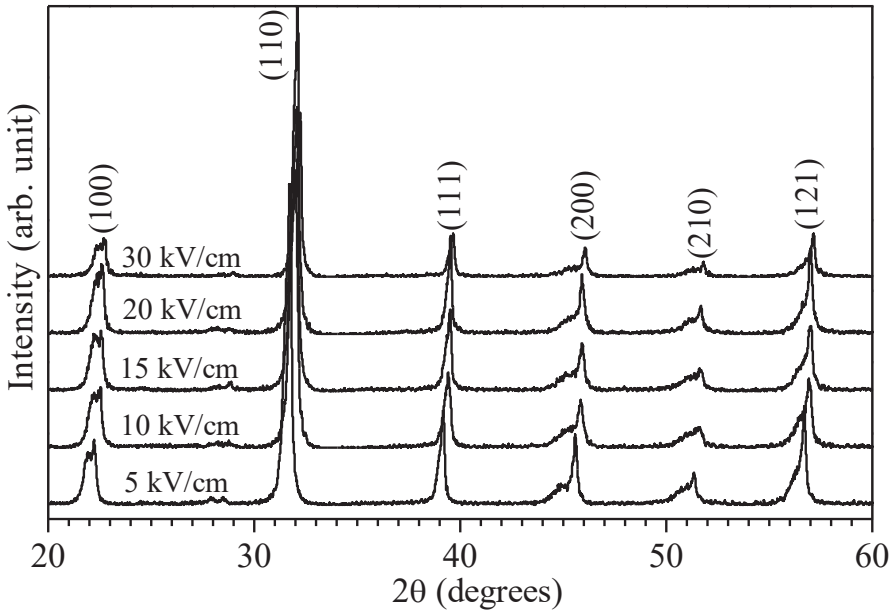

Fig.4.3 Evolution of XRD profiles for poled 0.65BNT-0.35PT samples at different poling field. The indices shown above the peaks correspond to pseudocubic structure.

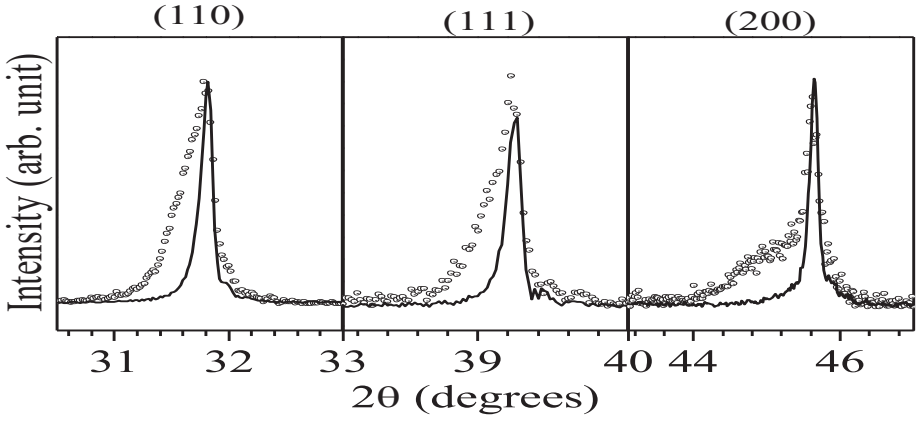

Fig.4.4 A Comparison of (110), (111) and (200) XRD profiles for unpoled (continuous line) and poled (scattered) at 20kV/cm sample of 0.65BNT-0.35PT. Indices shown above the peaks correspond to pseudocubic structure.

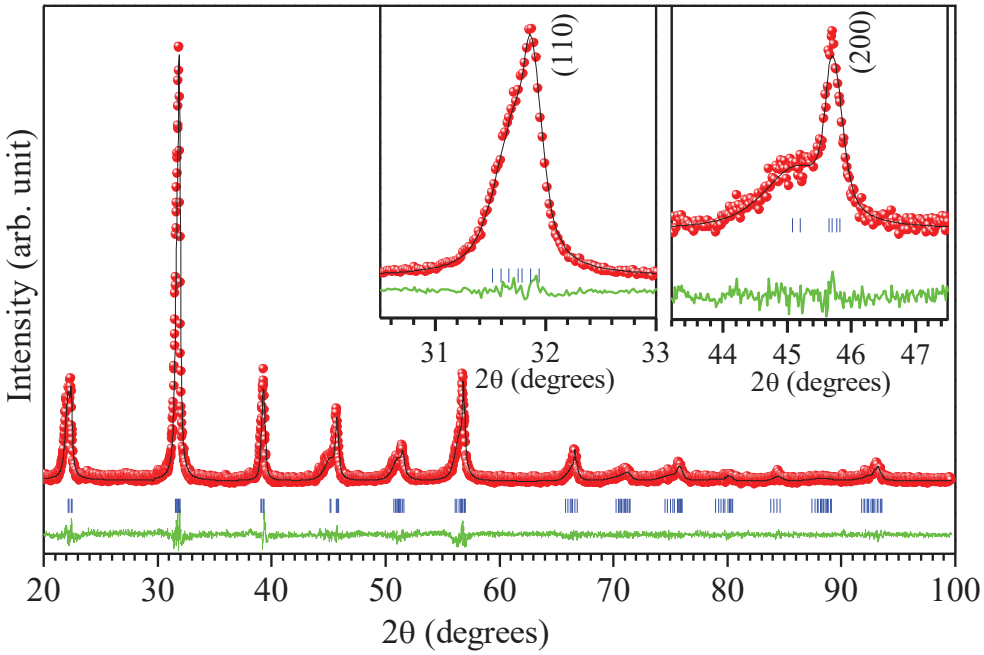

Fig.4.5 Experimentally observed (dots), theoretically calculated (continuous line) and their difference XRD (continuous bottom line) profiles for 0.65BNT-0.35PT ceramic poled at 15kV/cm obtained after Rietveld analysis of the powder XRD data using monoclinic (Pm) structure. The vertical tick-marks above the difference plot show the peak positions. Inset shows the goodness of fit for (110) and (002) pseudocubic reflections.

The most satisfactory fit between the observed and calculated profiles is obtained for the Pm space group. Fig.4.5 depicts the experimentally observed, theoretically calculated and difference XRD profiles in the 2θ range 20^0-100^0 for 0.65BNT-0.35PT sample poled at 15kV/cm. As can be seen from this figure, the fit is quite satisfactory. The variation of lattice parameter with poling field for 0.65BNT-0.35PT using monoclinic Pm space group is plotted in Fig.4.6. The lattice parameters "c", "b" and monoclinic angle (β) show slightly increasing trend with increasing the field strength, which suggests that the monoclinic distortion of the unit cell is increasing at higher poling fields. Insets of Fig.4.6 depict the variation of c-axis strain and unit cell volume, respectively, with poling field (E). The c-axis strain abruptly increases upto 1.14% under the applied poling field of 5kV/cm which gradually increases upto 1.6% at the poling field of 30kV/cm. The large strain results from the electric field induced pseudocubic to monoclinic phase transition. A similar strain jump is reported in PZN-PT [Durbin et al. (1999)] and PMN-PT [Fu and Cohen (2000)] subjected to external electric field. Park and Shrout (1997) have reported that in single crystal 0.92PZN-0.08PT ultrahigh strain (1.7%) could be achieved at the electric field strength of 120kV/cm [Park and Shrout (1997)]. In the present investigation, the strain level of ~ 1.6% is obtained at significantly lower field strength (~ 30kV/cm). It should be noted that 1.6% strain reported here is the microscopic lattice strain along c-axis. The strain is expected to be lower in polycrystalline ceramic samples. However, in single crystal sample, one may expect to get this

level of strain along c-axis at microscopic as well as macroscopic level. As shown in the inset of Fig.4.6, the unit cell volume (V) also shows a jump with increasing poling field in the beginning (~ 10kV/cm) and then levels off at higher fields. Significant increase in the unit cell volume is obtained due to the growth of the ferroelectric order during pseudocubic to monoclinic phase transition. The field induced transformation is not reversible in our ceramic BNT-PT sample. Removing the poling field does not revert back the original phase and crystal properties. So, the properties of the system completely changes after poling. A similar type of irreversible phase transformation is observed in the lead free system KNBT [Royles et al. (2010); Lee et al. (2011)] also. However, reversible and irreversible both types of transformations are observed in PMN-PT single crystals. On removing the poling field PMN-(0.28-0.30)PT single crystals revert back to initial rhombohedral phase while 0.68PMN-0.32PT single crystals remains in new orthorhombic phase and the actual initial properties are not restored [Shanthi and Lim (2009)]. Meanwhile, on heating the poled pellets of our system BNT-PT with x=0.35 at 500^0C for 30 minutes dipoles rearrange them in random directions and it revert back to initial cubic phase. Similar type of phase reversal to cubic phase was observed on crushing the poled pellets of BNT-PT with x=0.35.

4.3.3. Structure of 0.57BNT-0.43PT Poled at 20kV/cm

Similar to pseudocubic composition (x=0.35) of BNT-PT, the monoclinic composition (x=0.43) also shows the significant structural changes after electric field poling. A Comparison of XRD profiles for unpoled and poled (at 20kV/cm)

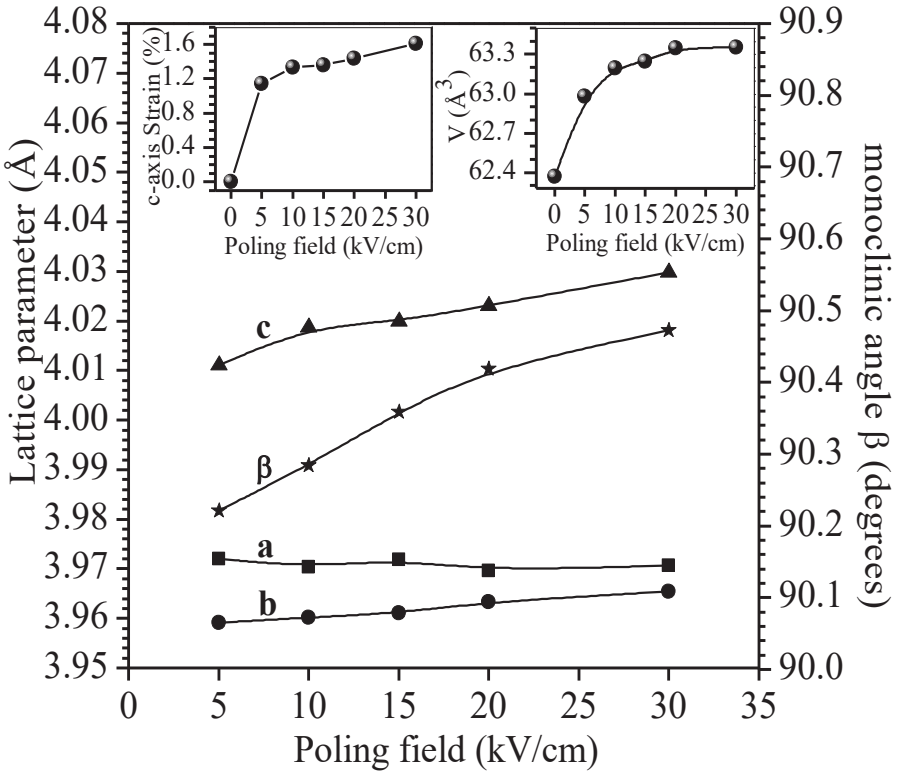

Fig.4.6 Variations of lattice parameter with poling field for 0.65BNT-0.35PT ceramic. Figures in the inset show the variation of c-axis microscopic lattice strain (%), and unit cell volume (V), with poling field (E) for 0.65BNT-0.35PT ceramic.

samples of 0.57BNT-0.43PT ceramics is shown in Fig.4.7. Significant change in the splitting and intensity of the XRD profiles is seen after poling in this figure. The intensity of (001) and (002) reflections have increased significantly while (100) and (200) have decreased after poling. This suggests that significant domain reorientation along c-direction takes place after electric field poling. The (001) and (002) profiles are also seen to be shifted on the lower 2θ side after poling while (100) and (200) remains nearly unaffected. This suggests that the c-axis has got elongated after poling. Fig.4.8 shows the Rietveld fit for of BNT-0.43PT pellet poled at 20kV/cm. Satisfactory fit between observed and calculated profiles were obtained after using coexistence of monoclinic (Pm) and tetragonal (P4mm) phases. This suggests that the MPB is shifting to the lower composition side in the electrically poled samples than that of the unpoled samples. Change in the location of MPB, which contain the rhombohedral (R3m) and monoclinic (Pm) phases is also reported in the lead based well-known system (1-x)$Pb(Mg_{1/3}Nb_{2/3})O_3$-x$PbTiO_3$, after the application of electric field. The shift in the MPB was observed towards the lower content of $PbTiO_3$ for which the rhombohedral compositions before poling appear as monoclinic compositions due to overlapping of domains [Bokov and Ye (2008)]. The rhombohedral 0.8$Na_{0.5}Bi_{0.5}TiO_3$-0.2$K_{0.5}Bi_{0.5}TiO_3$ is reported to transform into mixture of rhombohedral and tetragonal phases at applied electric field of strength more than 20kV/cm [Royles et al. (2010)]. The refined lattice parameters of 0.57BNT-0.43PT ceramic poled at 20kV/cm is listed in Table 4.1.

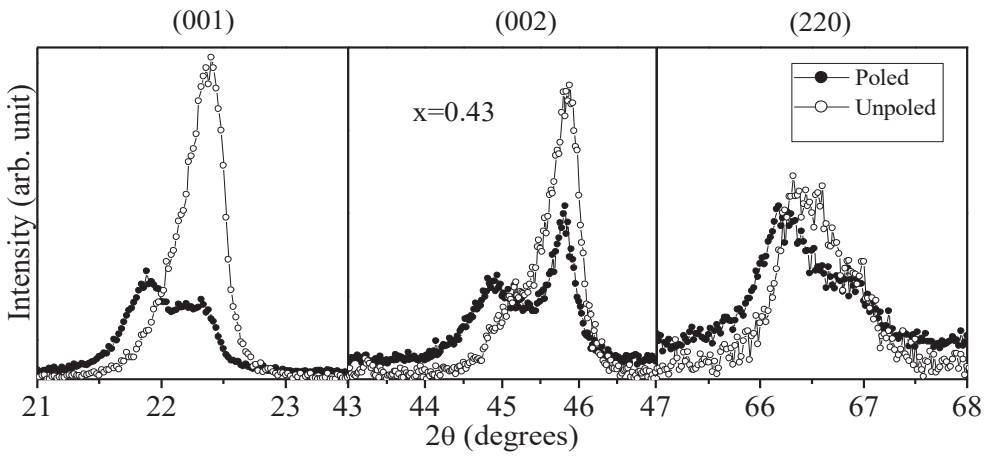

Fig.4.7 A Comparison of (001), (002) and (220) XRD profiles for unpoled and poled (at 20kV/cm) sample of 0.57BNT-0.43PT ceramics. Indices shown above the peaks correspond to pseudocubic structure.

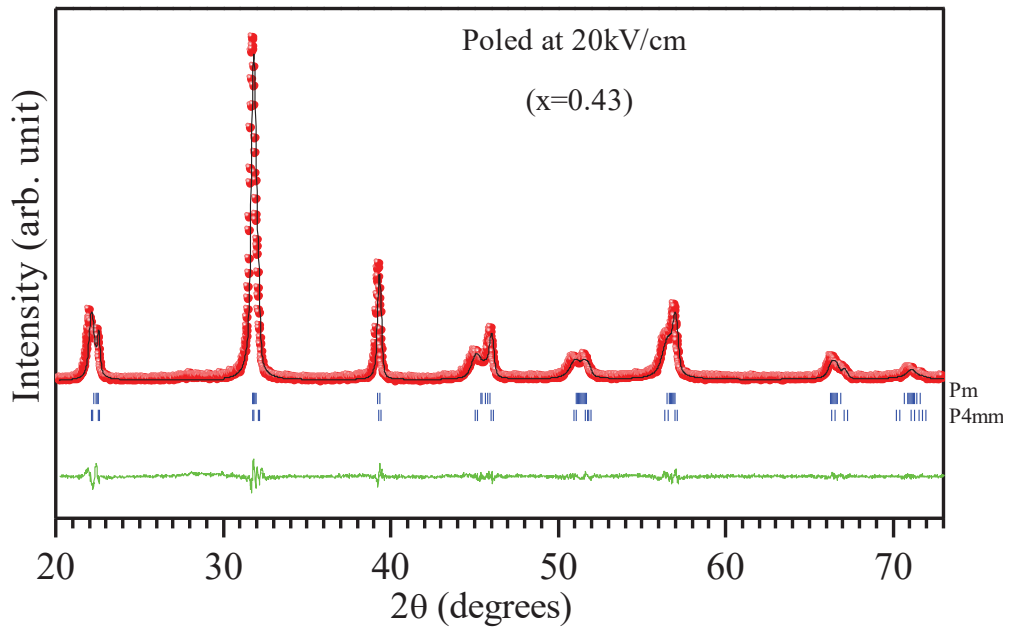

Fig.4.8 Experimentally observed (dots), theoretically calculated (continuous line) and their difference (continuous bottom line) profiles for 0.57BNT-0.43PT ceramic poled at 20kV/cm obtained after Rietveld analysis of the powder XRD data using monoclinic (Pm) and tetragonal (P4mm) Space groups. The vertical tick-marks above the difference plot show the peak positions.

4.3.4. Structural Changes in Tetragonal Composition after Poling

The tetragonal composition (x=0.50) also shows significant structural changes after poling. Fig.4.9 shows a comparison of XRD profiles for unpoled and poled (at 20kV/cm) sample of 0.50BNT-0.50PT ceramics. It is evident from Fig.4.9 that the intensity of (001), (002) and (202) profiles increases significantly for the poled sample in comparison to the intensity of the same peaks in unpoled samples. However, the intensity of (100), (200) and (220) profiles decreases for the poled sample in comparison to the intensity of the same peaks in unpoled samples. This clearly suggests that a large population of domains from a-direction get oriented along c-direction after poling for the tetragonal composition with x=0.50. The (002) profile shifts to lower 2θ side while (200) profile has got shifted to higher 2θ side after poling. This suggests that c-axis has got increased and a-axis has got contracted after poling resulting in the larger tetragonality. Similar types of domain texturing are reported by Tutuncu et al. (2014) in BNT-0.45PT. It has been shown by these authors [Tutuncu et al. (2014)] that the strong exchange of intensity of the tetragonal (002) and (200) Bragg reflections indicate the 90^0 domain wall reorientation in tetragonal structure. Rietveld profile matching for the poled sample of 0.50BNT-0.50PT is shown in Fig.4.10. Good fit between observed and calculated profiles was obtained using the tetragonal structure with space group P4mm. The refined lattice parameters of 0.50BNT-0.50PT ceramic poled at 20kV/cm is listed in Table 4.1 using tetragonal space group P4mm.

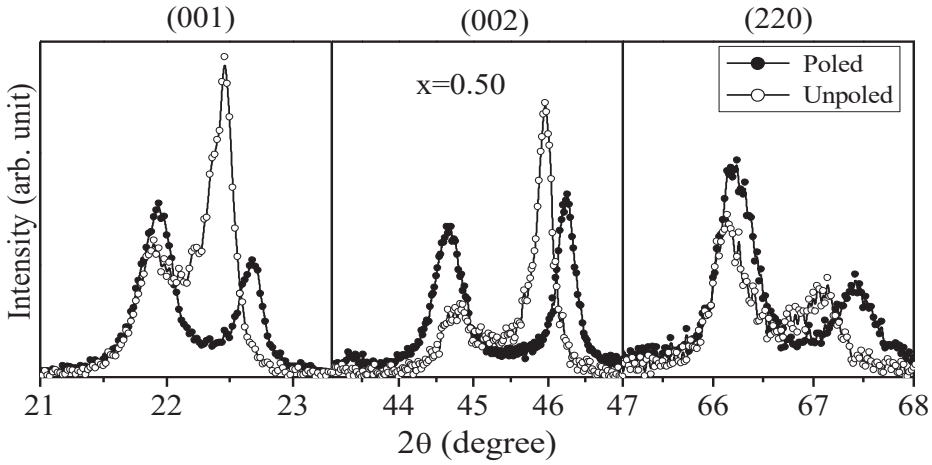

Fig.4.9 A Comparison of XRD profiles for unpoled and poled (at 20kV/cm) samples of 0.50BNT-0.50PT ceramics. Indices shown above the peaks correspond to pseudocubic strucutre.

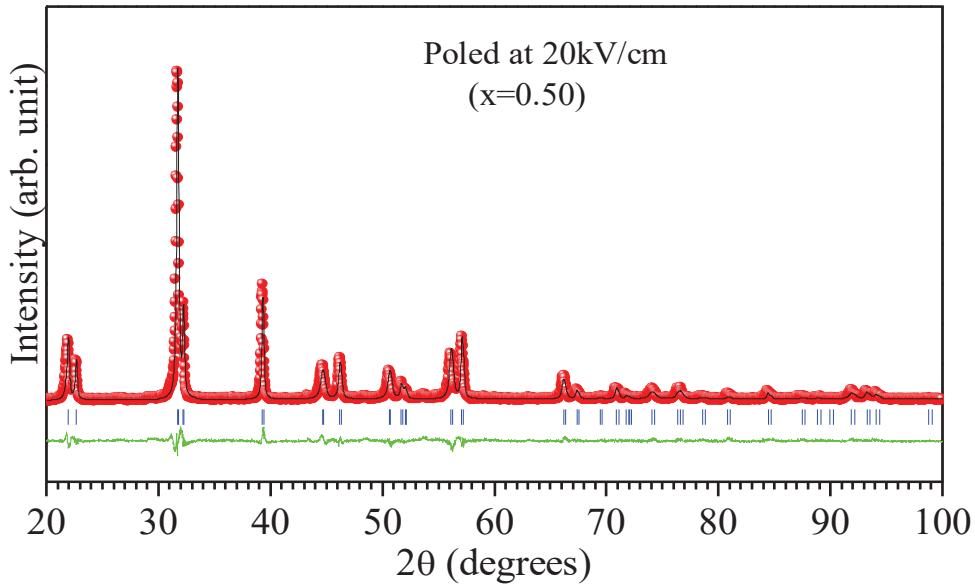

Fig.4.10 Experimentally observed (dots), theoretically calculated (continuous line) and their difference (continuous bottom line) profiles for 0.50BNT-0.40PT ceramic poled at 20kV/cm obtained after Rietveld analysis of the powder XRD data using tetragonal (T) P4mm space groups. The vertical tick-marks above the difference plot show the peak positions.

Table.4.1. Refined lattice parameters obtained by Rietveld profile matching for BNT-PT composition with x=0.43 using monoclinic (Pm) + tetragonal (P4mm) structure and x=0.50 using tetragonal (P4mm) structure, poled at 20kV/cm.

(x)	Space group	Lattice parameters (Å) (**poled**)	Lattice parameters (Å) (**unpoled**)
0.43	Pm	a=3.9665(3), b=3.9625(1) c=4.0827(1), β=90.084(2)^0	a=3.9649(5), b=3.9507(3) c=3.9883(5), β=90.113(4)^0
	P4mm	a=3.9507(2), c=4.0423(2)	a=3.9410(3), c=4.0283(5)
0.50	P4mm	a=3.9305(2), c=4.0601(2)	a_t=3.9351(3), c_t=4.0416(2)

4.3.5. P-E hysteresis Loop for BNT-PT

In order to see the effect of electric field, we carried out Polarization-electric field (P-E) hysteresis measurements on various compositions of BNT-PT. P-E hysteresis loops for the compositions with x=0.35 (cubic), 0.43 (monoclinic+tetragonal), 0.49 (monoclinic+tetragonal) and 0.55 (tetragonal) are shown in Figs.4.11(a-d), respectively. As can be seen from Fig.4.11(a), a well-saturated hysteresis loop with very high polarization is observed for x=0.35. Since the structure of this composition is cubic at room temperature, the hysteresis loop should not be obtained if it is the centrosymmetric paraelectric phase. This anomalous result could be explained only taking into account the relaxor ferroelectric behaviour of this composition.

In fact, temperature dependence of the dielectric permittivity for the composition with x=0.35 (discussed in Chapter V) exhibits a strong peak ~ 290^{0}C ($T_m^/$) with large frequency dispersion suggesting the presence of strong

relaxor features. In canonical relaxor $Pb(Mg_{1/3}Nb_{2/3})O_3$ (PMN), it has been reported that the average structure remains cubic down to 4K [Mathan et al. (1991)] because of the fact that the development of long range ferroelectric order is prevented by the presence of the quenched random fields [Westphal et al. (1992)] resulting from the presence of off-valent Mg^{2+}/Nb^{5+} ions at the B-site. However, the temperature dependence of the dielectric permittivity exhibits a strong peak with huge dielectric permittivity and frequency dispersion at 290K. Recently, in the case of PMN [Fu et al. (2009)], it has been reported that a well-saturated hysteresis loop similar to normal ferroelectrics is observed when the temperature is lowered below the freezing temperature (T_{vf}=220K) [Colla et al. (1995), Viehland et al. (1991)]. To verify a similar origin of the saturated hysteresis loop in cubic compositions of BNT-PT also, we have studied the temperature variation of permittivity for the composition with x=0.35 which is discussed in Chapter V. We observed that the freezing temperature (T_{vf}) for 0.65BNT-0.35PT is well above room temperature, therefore the saturated hysteresis loop may appear in average cubic symmetry similar to PMN [Fu et al. (2009)]. More surprisingly, the hysteresis loops shown in Figs. 4.11(b-d) for the two phase (x=0.43 and 0.49) and tetragonal phase (x=0.55) are slim in comparison to that for x=0.35. It seems that the reorientation of the nanodomains in relaxor compositions occur much more easily than the microscopic domains in the MPB and tetragonal compositions. Similar types of result are reported by Pandey et al. [Pandey et al. (2014)] in BMZ-PT, also.

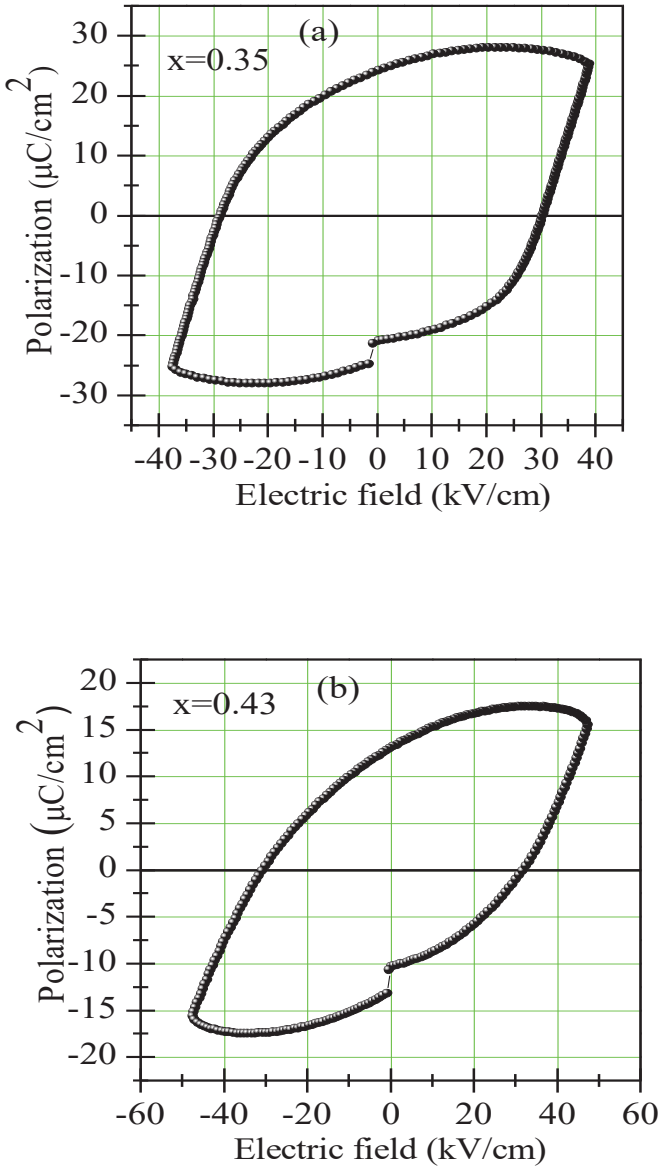

Fig.4.11. P-E hysteresis loop for BNT-xPT compositions with (a) x=0.35 and (b) 0.43.

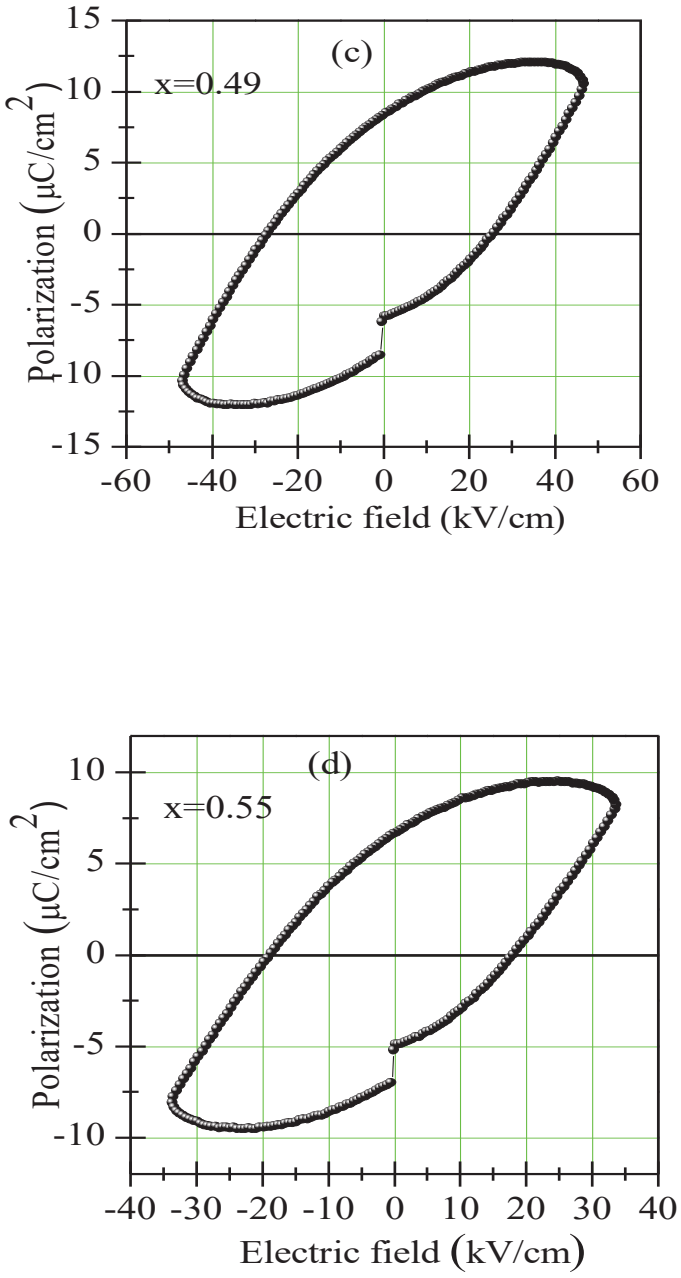

Fig.4.11. P-E hysteresis loop for BNT-xPT compositions with (c) x=0.49 and (d) 0.55.

4.4. Discussion

Recently, electric field induced phase transitions have been investigated in several ferroelectric solid solutions. In the lead free (Na,K)(Nb,Sb)O_3-$LiTaO_3$-x$BaZrO_3$ ceramics, the structure and physical properties are changed on the application of electric field. Before poling the structure is Tetragonal (T) +Rhombohedral (R) around the MPB composition. On application of the electric field, a new (orthorhombic) phase is induced inside the MPB region. The dielectric constant shows two peaks before poling corresponding to R-T-C phase transitions which turn into four peaks after the application of electric field corresponding to R-O-T-C phase transitions [Fu et al. (2012)]. Rao and Ranjan (2012) have shown that the electric-field induced transformation from monoclinic (Cc) to rhombohedral (R3c) structure takes place in lead free $Na_{1/2}Bi_{1/2}TiO_3$. 'Ba' substituted lead free $Na_{1/2}Bi_{1/2}TiO_3$ (i.e. $(Na_{1/2}Bi_{1/2})_{1-x}Ba_xTiO_3$) also exhibit the field induced phase transitions [Craciun et al. (2012)]. The splitting of (111) and (200) pseudocubic reflections increase with application of the electric field of strength 30kV/cm. It has been reported that the location of MPB can also get affected by appling the electric field in $Bi_{1/2}Na_{1/2}TiO_3$-$BaTiO_3$ solid solution [Ma et al. (2012)]. Field induced phase transition is also reported in lead based systems such as $Pb(Mg_{1/3}Nb_{2/3})O_3$ [Calvarin et al. (1995), Arndt et al. (1988)], $PbZr_{1-x}Ti_xO_3$ etc. [Guo et al. (2000)], $0.92Pb(Zn_{1/3}Nb_{2/3})O_3$-$0.8PbTiO_3$ [Durbin et al. (1999)]. Thus, the electric field induced phase transition is a common feature of the MPB ceramics for the compositions close to MPB

where the phase stability is very sensitive to small stimulant like electric field, pressure or compositional change.

In the lead free (1-x)(Na,K)(Nb,Sb)O_3-x$LiTaO_3$ solid solution, the structure and physical properties are reported to change on the application of electric field [Zuo et al. (2012)]. Rao and Ranjan (2012) have shown that electric-field induced transformation from monoclinic (Cc) to rhombohedral (R3c) structure is observed in lead free $Na_{1/2}Bi_{1/2}TiO_3$ after poling. Recently, domain wall reorientation has been investigated with significant change in the intensity of XRD profiles under applied electric field in 0.55BNT-0.45PT [Tutuncu et al. (2014)]. Electric field induced phase transitions from rhombohedral (R3c) to tetragonal phase is reported in $(Na_{0.5}Bi_{0.5})_{1-x}Ba_xTiO_3$ [Craciun et al. (2012)]. Ma et al. (2012) have shown that the compositional width of the MPB can be modified by applying the electric field in (1-x)$Bi_{0.5}Na_{0.5}TiO_3$-x$BaTiO_3$ solid solution. Electric field induced phase transformations and profile modification similar to BNT-PT is also reported in 0.93BNT- 0.07BT ceramic [Daniels et al. (2009)].

4.5. Summary

Appearance of piezoelectric response and structural modifications after poling are direct evidence of electric field induced phase transition in cubic 0.65BNT-0.35PT ceramic. The centrosymmetric cubic ($Pm\bar{3}m$) phase transforms into non centrosymmetric monoclinic (Pm) phase after poling. Electric field induced structural changes are also observed in the monoclinic (x=0.43) and tetragonal compositions (x=0.50). Significant domain reorientation is found after

poling in these compositions but phase coexistence also appears after poling in 0.57BNT-0.43PT. This suggests that MPB is shifted to lower composition side after electric poling. The present results reveal an unusually strong domain wall reorientation in the MPB and tetragonal phase during poling.